ACS APPLIED MATERIALS & INTERFACES

Letter

www.acsami.org

Ultrathin Wrinkled N-Doped Carbon Nanotubes for Noble-Metal Loading and Oxygen Reduction Reaction

Jiehua Liu,*[,†] Anli Shen,[‡] Xiangfeng Wei,[†] Kuan Zhou,[†] Wei Chen,[†] Fang Chen,[†] Jiaqi Xu,[†] Shuangyin Wang,*[,‡] and Liming Dai*[,§]

[†]Future Energy Laboratory, School of Materials Science and Engineering, Hefei University of Technology, 193 Tunxi Road, Hefei, Anhui 230009, China

[‡]State Key Laboratory of Chem/Bio-Sensing and Chemometrics, College of Chemistry and Chemical Engineering, Hunan University, Changsha 410082 P.R. China

[§]Department of Macromolecular Engineering, Case Western Reserve University, Cleveland, Ohio 44106, United States

Supporting Information

ABSTRACT: We describe the fabrication of ultrathin wrinkled N-doped carbon nanotubes by an in situ solid-state method. The positions of Co catalyst were first labeled by good-dispersion and highly loaded Au and Pt, indicating the most of Co are unsealed. The resultant unique nanoarchitecture, which exhibits the features of carbon nanotube and graphene with a combined effect of 1D and 2D carbon-based nanostructures, exhibited a superior ORR activity to carbon nanotubes and graphene. Moreover, the novel catalysts showed a better durability and higher tolerance to methanol crossover and poisoning effects than those of Pt/C.

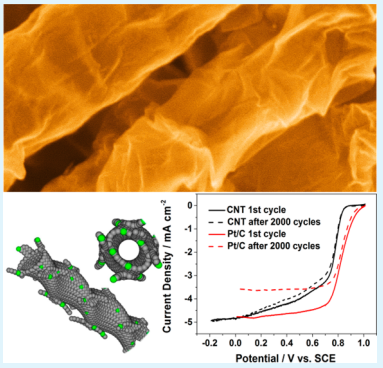

KEYWORDS: *fuel cells, non-noble catalysts, ultrathin carbon, electrocatalysis, oxygen reduction reactions, synergistic effect*

Nanoarchitectures provide a powerful impetus to the development of novel high-performance materials in energy storage and conversion.[1,2] Because of their unique surface and structural properties, carbon-based nanoarchitectures have attracted a great deal of interest as catalysts in fuel cells and rechargeable batteries.[3,4] In fuel cells, various nano/microarchitectures were successfully prepared, such as Pt/hollow carbon nanospheres,[5,6] Pt/carbon nanotubes (CNTs),[7,8] Pt/graphene,[9,10] and Pt-based alloys.[11,12] Although Pt and its alloys exhibit superior catalytic activities for oxygen reduction reaction (ORR), their high cost, poor stability, and poor poisoning effect still limited their application in commercial fuel cells. Therefore, the development of Pt-free electrocatalysts as substitutes for Pt-based electrocatalysts is of essential importance.

Recently, various metal-free carbon-based electrocatalysts have been demonstrated to exhibit high electrocatalytic activity for ORR and their catalytic mechanisms have been successfully proved by experiments and theoretical simulation.[13−15] Heteroatom (N, B, P, O, and/or S)-doped carbon electrocatalysts have shown advanced activities because of the doping-induced charge polarization.[16,17] According to a pioneering report, vertically aligned N-doped CNTs (NCNTs) exhibited superior performance to Pt/C.[18] N-doped single walled CNTs also showed good electrocatalytic performance.[19] Besides, two-dimensional heteroatom-doped carbon (e.g., graphene) can also exhibit good catalytic performance for ORR.[20,21] Indeed, N-doped graphene also shows enhanced catalytic activity for ORR.[22,23]

There are three most important requirements for highly efficient ORR catalysts, including amounts of electrocatalytic sites, good conductivity for electron transfer, and open paths for reactant/electrolyte diffusion. Single-walled CNTs can expose many active sites, but the reactant/electrolyte diffusion in its small internal channel is often limited and the intertube conductivity may be low (Figure 1a). Figure 1b shows N-doped graphene sheet with the desired active sites, but unfortunately, the layer-by-layer stacking may cause a significant loss of the active sites and increase in the interface resistance to the electron/electrolyte transport in the 2D structure. Although MWCNTs could enhance electron transfer with respect to SWCNTs and layer-by-layer stacked graphene, their low surface area may limit the catalytic activity, particularly when their diameter is >50 nm (Figure 1c). Therefore, it is necessary to explore novel nitrogen-doped carbon nanostructures with more catalytic sites and facilitated electron/electrolyte transport paths.

Received: August 16, 2015
Accepted: September 10, 2015
Published: September 10, 2015

DOI: 10.1021/acsami.5b07554
ACS Appl. Mater. Interfaces 2015, 7, 20507−20512

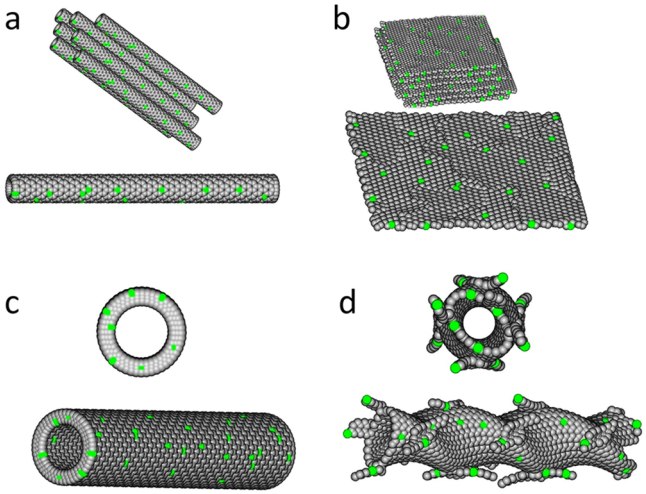

Figure 1. (a) Nitrogen-doped single-walled CNTs; (b) nitrogen-doped graphene; (c) nitrogen-doped multiwalled CNTs; and (d) nitrogen-doped few-layered distorted CNTs.

A proposed CNT-based structure is shown in Figure 1d, which combines NCNTs with few-layer 2D graphene thickness. In this proposed structure, ultrathin wrinkled walls may provide more ORR catalytic sites and its large diameter could improve the electrical conductivity of the novel structure by reducing the interface resistance. Our previous results indicated that the edge of carbon catalysts have superior ORR activity than that in basal plane.[24] Calculations also demonstrated that N-doped carbon catalysts may offer good active sites at Stone−Wales defect and provide tuned ORR activity by the curvature around the active site based on the first-principle methods.[25] Therefore, the designed advanced structure would be able to show superior ORR activity and quickening electron transfer because of a combined effect of carbon materials with different dimensions. The large-diameter hollow core should also facilitate the electrolyte transport.

In this work, we developed the in situ fabrication of ultrathin wrinkled NCNTs fabricated by a solid catalysis route. The novel structure exhibited excellent catalytic performance as an efficient ORR electrocatalyst. In brief, the carbon materials were prepared using a facile in situ solid-state reaction involving polymerization and self-catalytic synthesis of CNTs with Co catalyst (see the Supporting Information for more details). Electrochemical results showed the ultrathin wrinkled NCNTs have ideal electrocatalytic activities with a good durability, and superior tolerance and poisoning effects to Pt/C electrocatalyst. The novel structure possesses the features of graphene and CNTs that improved ORR activity.

N-doped carbon materials often employed urea, melamine, and their derivatives as carbon and nitrogen sources because of their low cost, abundance, and nonflammability. In this work, we also use melamine as starting materials and cobalt acetate tetrahydrate as catalyst precursor to prepare N-doped materials in a facile self-catalytic method. It is to be observed that the low pressure (below −0.5 atm) and the amount of Co are key conditions to obtain the unique N-doped carbon materials at 650 °C, much lower than reported reaction temperatures of 900 °C or higher in Table S1. More details are provided in

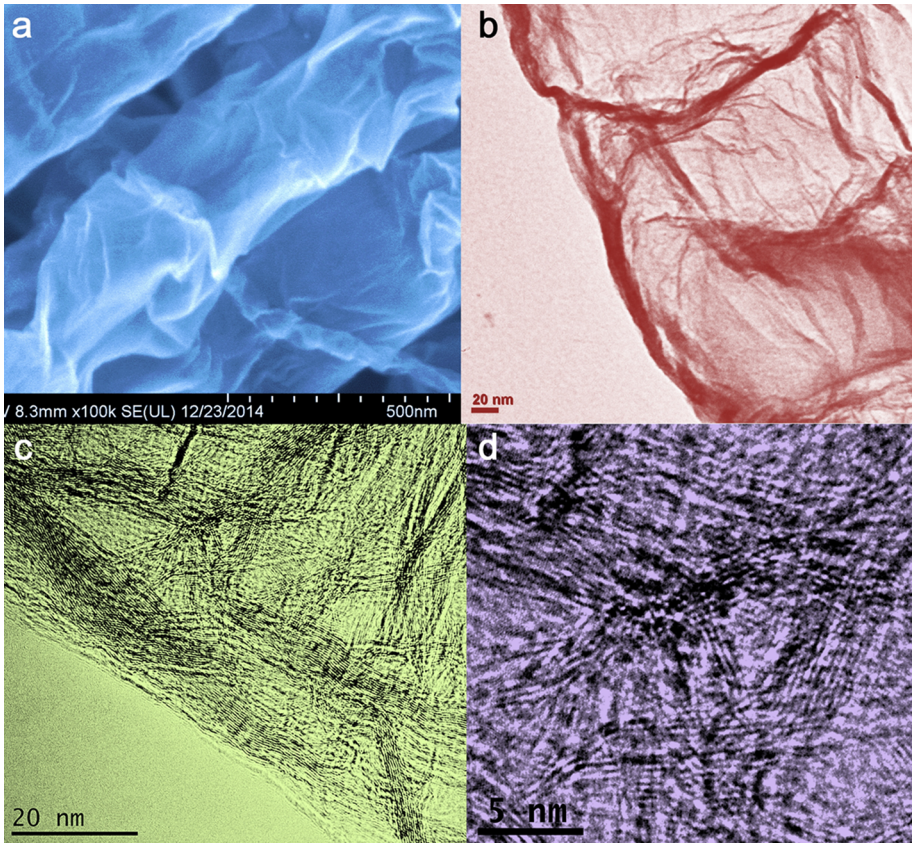

Figure 2. Morphologies of ultrathin distorted carbon nanotube obtained at 650 °C and Co catalyst removed. (a) FESEM image of CNT-650; (b) TEM image of CNT-650 obtained at 100 kV; (c) TEM and (d) HRTEM images of CNT-650 obtained at 200 kV.

DOI: 10.1021/acsami.5b07554
ACS Appl. Mater. Interfaces 2015, 7, 20507−20512

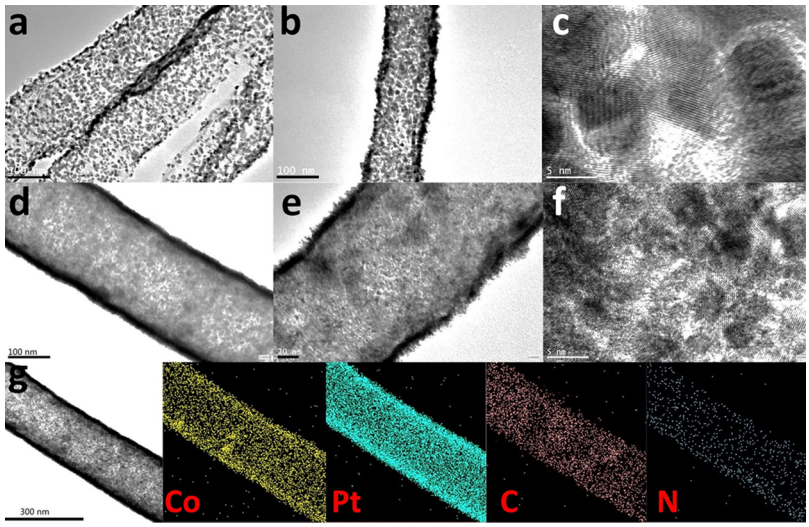

Figure 3. High noble metal-loaded CoCNTs obtained at 650 °C. (a, b) TEM images and (c) HRTEM image of 25 wt % Au/CoCNTs; (d, e) TEM images and (f) HRTEM of 30 wt % Pt/CoCNTs; (g) STEM and elemental mappings (Co, Pt, C, N) of 30 wt % Pt/CoCNTs.

Supporting Information. The as-synthesized sample at 650 and 700 °C were named CoCNT-650 and CoCNT-650. After Co catalyst was removed, the materials were entitled CNT-650 and CNT-700, respectively.

The morphologies of the obtained materials were first collected by electron microscopy (EM) analysis including FESEM and TEM. In Figure 2a, FESEM image shows that CNT-650 consists of CNTs with a corrugated surface and a large channel size of 100−300 nm, and FESEM image at low magnification displays the length of more than 5 μm in Figure S1. To observe its surface and thickness, TEM images were collected at 100 kV. Figure S2 shows the tubelike structure with ultrathin wall. Figure 2b is an enlarged TEM image which also exhibits the unique wrinkled surface of CNT-650. TEM images of CNT-650 were collected at a higher voltage of 200 kV to confirm the structure. Figure S3 shows the same tubelike structure as observed in Figure S2. Different from the conventional CNTs, the CNT-650 has a large channel diameter, ultrathin wall and corrugated surface. HRTEM images are also collected to check the corrugated wall in Figure 2c, d. As shown in Figure 2c, the thickness of wall of CNT-650 is only few nanometres. In Figure 2d, we can further find the wall consisting of few-layer graphene, which may exhibit good catalytic activity for ORR. When synthesized at 700 °C, the CoCNT-700 also retains the unique structure as shown in Figure S4.

The crystal structures of as-obtained materials were studied by powder X-ray diffraction (XRD) analysis. The XRD pattern of CoCNT-650 shows metal Co exists in the sample (Figure S5). In Figure S6, the peak at 26.4° of CNT-650 comes from (002) of graphite and agrees well with the above HRTEM results. On the other hand, the peak height increases significantly on account of improved degree of graphitization by elevating the reaction temperature from 650 to 700 °C. Raman spectra were also recorded to study the electronic properties structure of the prepared CNTs. The typical bands (D and G) at 1348 and 1587 cm^{-1} represent the defect-C and the graphitic-C respectively as shown in Figure S7. The I_G/I_D ratio markedly increases from 1.08 to 1.30 when the synthesis temperature increases in good consistence with XRD results.

Surface features of CNT-650 were analyzed by using N_2 sorption test at 77 K. Brunauer−Emmett−Teller surface area of CNT-650, which is derived from its N_2 sorption isotherms in Figure S8, is up to 94.7 m^2 g^{-1}, larger than of common MWCNTs (<50 m^2 g^{-1}) with a diameter of 100 nm reported previously.[26] CNT-650 with a high surface area could present abundant catalytic sites for ORR. The surface area distribution curve (inset of Figure S8b) demonstrates that the area in a range from 3 to 8 nm is associated with the corrugated surface of CNT-650, which is supported by the TEM analysis.

X-ray photoelectron spectroscopy (XPS) experiments are used to detect the main compositions of CNT-650. Full XPS curve of CNT-650 is given in Figure S9 and presents that carbon, nitrogen and oxygen are the main components. It should be mentioned that nitrogen content is 2.1 at % for the CNT-650 sample whereas cobalt is only 0.29 at %, indicating that trace Co exists in the ultrathin wall of NCNTs. Co residue is possibly coated completely by carbon and difficult to be removed. XPS spectra in high resolution were shown in Figure S10. N 1s XPS spectra were fitted into two main peaks at 398.5 and 401.2 eV for pyridine-N and graphitic-N microenvironments, respectively.

The possible growth mechanism is explored by in situ labeling for the unique CNT structure. Because metal Co is a reducing agent that can react with Au(III) to form Au or Au−Co alloy in situ, Au(III) can be used to label the position of cobalt. We herein use $AuCl_3$ to check the status of Co catalyst in CoCNTs. Figure S11 depicts the TEM images of CoCNT-650 with low Au loading of 5 wt %. Figure S11a shows the good-dispersion ultrafine Au nanoparticles could be obtained without any reduction reagent added indicating the part of Co^0 is not sealed in the CoCNTs. Figure S11b displays that the obtained nanoparticle is face-centered cubic Au with the (111) plane lattice spacing of 0.23 nm. To test the position of most Co, highly loaded Au is provided as a direct proof to prove the unencapsulated Co position in Figure 3a−c. Figure 3a, b shows typical TEM images of Au/CoCNT (Au ∼ 25 wt %) composite, which clearly display the Au deposit with ∼5 nm throughout CoCNTs. Cobalt has high dispersion in the CNT, especially on the surface. HRTEM analysis (Figure 3c) revealed the highly crystalline features of Au particles with a crystal size

DOI: 10.1021/acsami.5b07554
ACS Appl. Mater. Interfaces 2015, 7, 20507−20512

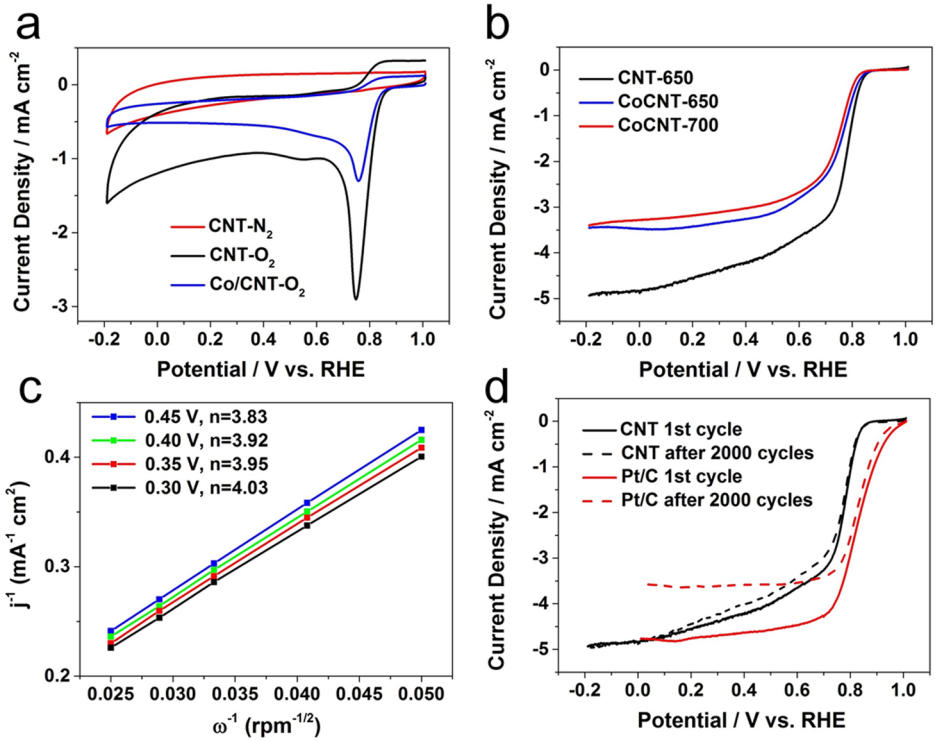

Figure 4. Electrochemical performances of electrocatalysts in 0.1 M KOH aqueous solution. (a) Typical cyclic voltammograms at the electrodes of CNT-650 and CoCNT-650 in a N_2/O_2-saturated conditions; (b) RDE voltammograms of CNT-650, CoCNT-650, and CoCNT-700 electrodes in an O_2-saturated conditions at 1600 rpm; (c) K–L plots of CNT-650 at 0.45, 0.40, 0.35, and 0.30 V; (d) LSV plots of CNT-650 and Pt/C at initial cycle and after 2000 cycles at 1600 rpm, respectively.

of ~5 nm. This suggests that Co had enough reducing ability to convert the Au(III) precursor into Au. To the best of our knowledge, a uniform dispersion of ultrafine nanoparticles onto the entire region of the CNT support was realized in situ without any additional reducing agents for the first time. It is worth noting that the Au particle size could be mediated while Au(III) ion content could be tuned as wish.

We further prepared Pt/CoCNT composites using the same method to test its universal applicability. TEM images in Figure 3d–f illustrate highly loaded Pt (~30 wt %) on CoCNTs, which displays that numerous particles with an ultrafine size (3–6 nm) and a very narrow size distribution were coated on surface of CoCNTs. The crystal size of Pt in Pt/CoCNT-650 is ~5 nm using Scherrer equation based on XRD curve in Figure S12. We also examined the elemental mappings of Co, Pt, C, and N in Figure 3g, which are all uniformly distributed in Pt/CoCNTs, leading to the possible formation of Pt-shell nanotube structure. These results demonstrated that the good-dispersion Co might have encapsulated the N-doped CNTs structure. Unlike the reported Pt/CNTs catalysts with alcohols or polyols as reducing agents,[27,28] we do not use any additional reducing agent to prepare Pt/CoCNTs and Au/CoCNTs (Table S2). As a contrast, we also tested the Pt loaded on CNT-650 with ethylene glycol as reducing agent at 140 °C. The result shows uneven Pt distribution on CNT-650 in Figure S13.

Ultrathin wrinkled NCNTs are expected to speed up electron transfer and improve reaction rate by a combined effect of carbon materials of 1D and 2D architectures. Figure 4a shows the main reduction process of CNT-650 is at ~0.75 V, but there is no response in N_2-saturated condition. CNT-650 has a higher activity than N- or B–N-doped graphene-based electrocatalysts.[29,30] We attribute the improved performance to its high-efficient active sites associated with the ultrathin distorted structure. Moreover, CNT-650 with a large diameter may increase the conductivity of electrode. Although CoCNT-650 has a little positive potential centered at o.76 V due to the contribution of Co catalyst,[10] CNT-650 exhibits a superior activity to CoCNT-650. The possible reason is that CNT-650 offers more effective catalytic sites after Co removed than CoCNT-650.

Linear-sweep voltammetry (LSV) curves of distorted nitrogen-doped CNT-650, CoCNT-650 and CoCNT-700 are provided in Figure 4b. CNT-650 exhibits a good activity with a high onset potential at 0.87 V at 1600 rpm. CNT-650 also offers higher current density of 4.82 mA cm^{-2} than 3.48 and 3.28 mA cm^{-2} of CoCNT-650 and CoCNT-700 at 0 V, respectively. LSV curves of the CoCNT-650 exhibit a lower onset potential of 0.85 V than 0.87 V for CNT-650. Therefore, the novel metal-free structure contributes to the enhanced ORR activity, which is superior to the CoCNTs catalysts. In Figure 4c, the Koutecky–Levich (K–L) curves of CNT-650 suggest the first-order kinetics on CNT-650 for ORR. The transferred electron numbers (n) per O_2 molecule for CNT-650 are 3.82, 3.93, 3.95, and 4.03 at the potential of 0.45, 0.40, 0.35, and 0.30 V on the basis of LSV curves of distorted nitrogen-doped CNT-650 at different rotation speeds (Figure S14). Furthermore, cycling performances of commercial 20% Pt/C and N-doped CNT-650 were further investigated as shown in Figure 4d. At the first cycle, CNT-650 and Pt/C have close current densities of 4.81 and 4.77 mA cm^{-2} at 0 V, respectively. More importantly, the current density retention is nearly 100% for CNT-650 and only 79% for Pt/C at 0 V after 2000 cycles, indicating better stability of CNT-650 than Pt/C.

DOI: 10.1021/acsami.5b07554
ACS Appl. Mater. Interfaces 2015, 7, 20507–20512

To assess the tolerance of CNTs for methanol, CV curves were tested in O_2-saturated solutions with 0.1 M KOH and 1 M CH_3OH. There is a little change for CV curves of CNT-650 with and without 1 M methanol in Figure S15. Twenty wt % Pt/C was used in a comparative experiment under the same conditions (Figure S16). The results show that the current density (only 1.03 mA cm^{-2}) of Pt/C at 0.61 V is much lower than 2.96 mA cm^{-2} of CNT-650. Therefore, the ultrathin winkled NCNTs exhibit a superior methanol tolerance performance than Pt/C.

In conclusion, ultrathin wrinkled NCNTs were facile synthesized in situ using a facile solid-state method. The novel structure has ultrathin wall of 1−2 nm and wrinkled structure, providing a desired large interface. The Co catalysts were labeled with high-loaded Au and Pt in situ, indicating the most of Co are unsealed and can be almost removed. Electrochemical measurements showed that the unique features contributed to the enhancement of ORR activity, superior to common NCNTs and graphene, respectively. The ultrathin NCNTs exhibit an excellent electrocatalytic activity with better durability, and higher tolerance to CH_3OH crossover and poisoning effects than those of Pt/C. Furthermore, this work provides a universal strategy for developing good-dispersion and/or highly loaded metal/alloy−CNT composites as electrocatalysts in fuel cells.

■ ASSOCIATED CONTENT

Supporting Information

The Supporting Information is available free of charge on the ACS Publications website at DOI: 10.1021/acsami.5b07554.

Experiment section, TEM images, XRD curves, Raman curves, XPS spectra, additional electrochemical characterizations (PDF)

■ AUTHOR INFORMATION

Corresponding Authors

*E-mail: liujh@hfut.edu.cn.
*E-mail: shuangyinwang@hnu.edu.cn.
*E-mail: liming.dai@case.edu.

Notes

The authors declare no competing financial interest.

■ ACKNOWLEDGMENTS

This work was supported by Natural Science Foundation of China (21303038, 51402100), Scientific Research Foundation for the Returned Overseas Chinese Scholars, State Education Ministry, and One Hundred Talents Project of Anhui Province.

■ REFERENCES

(1) Liu, J. H.; Chen, J. S.; Wei, X. F.; Lou, X. W.; Liu, X. W. Sandwich-Like, Stacked Ultrathin Titanate Nanosheets for Ultrafast Lithium Storage. *Adv. Mater.* **2011**, *23* (8), 998−1002.

(2) Wei, X. F.; Liu, J. H.; Chua, Y. Z.; Song, J. L.; Liu, X. W. Fabrication of O (dye)-Terminated Anatase TiO_2 Nanosheets for Dye Sensitized Solar Cells. *Energy Environ. Sci.* **2011**, *4* (6), 2054−2057.

(3) Cheng, F.; Chen, J. Metal-Air Batteries: from Oxygen Reduction Electrochemistry to Cathode Catalysts. *Chem. Soc. Rev.* **2012**, *41* (6), 2172−2192.

(4) Suntivich, J.; Gasteiger, H. A.; Yabuuchi, N.; Nakanishi, H.; Goodenough, J. B.; Shao-Horn, Y. Design Principles for Oxygen-Reduction Activity on Perovskite Oxide Catalysts for Fuel Cells and Metal-Air Batteries. *Nat. Chem.* **2011**, *3* (7), 546−550.

(5) Wang, X.; Hu, C.; Xiong, Y.; Liu, H.; Du, G.; He, X. Carbon-Nanosphere-Supported Pt Nanoparticles for Methanol and Ethanol Electro-Oxidation in Alkaline Media. *J. Power Sources* **2011**, *196* (4), 1904−1908.

(6) Fang, B.; Kim, J. H.; Kim, M.; Yu, J.-S. Ordered Hierarchical Nanostructured Carbon as a Highly Efficient Cathode Catalyst Support in Proton Exchange Membrane Fuel Cell. *Chem. Mater.* **2009**, *21* (5), 789−796.

(7) Deng, D.; Yu, L.; Chen, X.; Wang, G.; Jin, L.; Pan, X.; Deng, J.; Sun, G.; Bao, X. Iron Encapsulated within Pod-like Carbon Nanotubes for Oxygen Reduction Reaction. *Angew. Chem., Int. Ed.* **2013**, *52* (1), 371−375.

(8) Liang, Y.; Wang, H.; Diao, P.; Chang, W.; Hong, G.; Li, Y.; Gong, M.; Xie, L.; Zhou, J.; Wang, J.; Regier, T. Z.; Wei, F.; Dai, H. Oxygen Reduction Electrocatalyst Based on Strongly Coupled Cobalt Oxide Nanocrystals and Carbon Nanotubes. *J. Am. Chem. Soc.* **2012**, *134* (38), 15849−15857.

(9) Jahan, M.; Bao, Q.; Loh, K. P. Electrocatalytically Active Graphene-Porphyrin MOF Composite for Oxygen Reduction Reaction. *J. Am. Chem. Soc.* **2012**, *134* (15), 6707−6713.

(10) Liang, Y.; Li, Y.; Wang, H.; Zhou, J.; Wang, J.; Regier, T.; Dai, H. Co_3O_4 Nanocrystals on Graphene as a Synergistic Catalyst for Oxygen Reduction Reaction. *Nat. Mater.* **2011**, *10* (10), 780−786.

(11) Bing, Y.; Liu, H.; Zhang, L.; Ghosh, D.; Zhang, J. Nanostructured Pt-Alloy Electrocatalysts for PEM Fuel Cell Oxygen Reduction Reaction. *Chem. Soc. Rev.* **2010**, *39* (6), 2184−2202.

(12) Cui, C.; Gan, L.; Heggen, M.; Rudi, S.; Strasser, P. Compositional Segregation in Shaped Pt Alloy Nanoparticles and Their Structural Behaviour during Electrocatalysis. *Nat. Mater.* **2013**, *12* (8), 765−771.

(13) Wood, K. N.; O'Hayre, R.; Pylypenko, S. Recent Progress on Nitrogen/Carbon Structures Designed for Use in Energy and Sustainability Applications. *Energy Environ. Sci.* **2014**, *7* (4), 1212−1249.

(14) Lu, X.; Chen, Z.; Schleyer, P. V. R. Are Stone−Wales Defect Sites Always More Reactive Than Perfect Sites in the Sidewalls of Single-Wall Carbon Nanotubes. *J. Am. Chem. Soc.* **2005**, *127* (1), 20−21.

(15) Ma, J.; Alfè, D.; Michaelides, A.; Wang, E. Stone-Wales Defects in Graphene and Other Planar sp^2-Bonded Materials. *Phys. Rev. B: Condens. Matter Mater. Phys.* **2009**, *80* (3), 033407.

(16) Zhao, Y.; Yang, L.; Chen, S.; Wang, X.; Ma, Y.; Wu, Q.; Jiang, Y.; Qian, W.; Hu, Z. Can Boron and Nitrogen Co-doping Improve Oxygen Reduction Reaction Activity of Carbon Nanotubes? *J. Am. Chem. Soc.* **2013**, *135* (4), 1201−1204.

(17) Meng, Y. Y.; Voiry, D.; Goswami, A.; Zou, X. X.; Huang, X. X.; Chhowalla, M.; Liu, Z. W.; Asefa, T. N-, O-, and S-Tridoped Nanoporous Carbons as Selective Catalysts for Oxygen Reduction and Alcohol Oxidation Reactions. *J. Am. Chem. Soc.* **2014**, *136* (39), 13554−13557.

(18) Gong, K.; Du, F.; Xia, Z.; Durstock, M.; Dai, L. Nitrogen-Doped Carbon Nanotube Arrays with High Electrocatalytic Activity for Oxygen Reduction. *Science* **2009**, *323* (5915), 760−764.

(19) Yu, D.; Zhang, Q.; Dai, L. Highly Efficient Metal-Free Growth of Nitrogen-Doped Single-Walled Carbon Nanotubes on Plasma-Etched Substrates for Oxygen Reduction. *J. Am. Chem. Soc.* **2010**, *132* (43), 15127−15129.

(20) Chen, P.; Wang, L.-K.; Wang, G.; Gao, M.-R.; Ge, J.; Yuan, W.-J.; Shen, Y.-H.; Xie, A.-J.; Yu, S.-H. Nitrogen-Doped Nanoporous Carbon Nanosheets Derived from Plant Biomass: An Efficient Catalyst for Oxygen Reduction Reaction. *Energy Environ. Sci.* **2014**, *7* (12), 4095−4103.

(21) Lai, L.; Potts, J. R.; Zhan, D.; Wang, L.; Poh, C. K.; Tang, C.; Gong, H.; Shen, Z.; Lin, J.; Ruoff, R. S. Exploration of the Active Center Structure of Nitrogen-Doped Graphene-Based Catalysts for Oxygen Reduction Reaction. *Energy Environ. Sci.* **2012**, *5* (7), 7936−7942.

(22) Sheng, Z. H.; Shao, L.; Chen, J. J.; Bao, W. J.; Wang, F. B.; Xia, X. H. Catalyst-Free Synthesis of Nitrogen-Doped Graphene via

DOI: 10.1021/acsami.5b07554
ACS Appl. Mater. Interfaces 2015, 7, 20507−20512

Thermal Annealing Graphite Oxide with Melamine and Its Excellent Electrocatalysis. *ACS Nano* **2011**, *5* (6), 4350−4358.
(23) Wang, D.-W.; Su, D. Heterogeneous Nanocarbon Materials for Oxygen Reduction Reaction. *Energy Environ. Sci.* **2014**, *7* (2), 576−591.
(24) Shen, A.; Zou, Y.; Wang, Q.; Dryfe, R. A. W.; Huang, X.; Dou, S.; Dai, L.; Wang, S. Oxygen Reduction Reaction in a Droplet on Graphite: Direct Evidence that the Edge Is More Active than the Basal Plane. *Angew. Chem., Int. Ed.* **2014**, *53* (40), 10804−10808.
(25) Chai, G.-L.; Hou, Z.; Shu, D.-J.; Ikeda, T.; Terakura, K. Active Sites and Mechanisms for Oxygen Reduction Reaction on Nitrogen-Doped Carbon Alloy Catalysts: Stone−Wales Defect and Curvature Effect. *J. Am. Chem. Soc.* **2014**, *136* (39), 13629−13640.
(26) O'Regan, B.; Lenzmann, F.; Muis, R.; Wienke, J. A Solid-State Dye-Sensitized Solar Cell Fabricated with Pressure-Treated P25−TiO_2 and CuSCN: Analysis of Pore Filling and IV Characteristics. *Chem. Mater.* **2002**, *14* (12), 5023−5029.
(27) Palaniselvam, T.; Irshad, A.; Unni, B.; Kurungot, S. Activity Modulated Low Platium Content Oxygen Reduction Electrocatalysts Prepared by Inducing Nano-Order Dislocations on Carbon Nanofiber through N_2-Doping. *J. Phys. Chem. C* **2012**, *116* (28), 14754−14763.
(28) Cheng, N.; Banis, M. N.; Liu, J.; Riese, A.; Li, X.; Li, R.; Ye, S.; Knights, S.; Sun, X. Extremely Stable Platinum Nanoparticles Encapsulated in a Zirconia Nanocage by Area-Selective Atomic Layer Deposition for the Oxygen Reduction Reaction. *Adv. Mater.* **2015**, *27* (2), 277−281.
(29) Ito, Y.; Qiu, H. J.; Fujita, T.; Tanabe, Y.; Tanigaki, K.; Chen, M. W. Bicontinuous Nanoporous N-doped Graphene for the Oxygen Reduction Reaction. *Adv. Mater.* **2014**, *26* (24), 4145−4150.
(30) Wang, S.; Zhang, L.; Xia, Z.; Roy, A.; Chang, D. W.; Baek, J.-B.; Dai, L. BCN Graphene as Efficient Metal-Free Electrocatalyst for the Oxygen Reduction Reaction. *Angew. Chem., Int. Ed.* **2012**, *51* (17), 4209−4212.

DOI: 10.1021/acsami.5b07554
ACS Appl. Mater. Interfaces 2015, 7, 20507−20512